

Article

Supercapacitive Performance of N-Doped Graphene/Mn₃O₄/Fe₃O₄ as an Electrode Material

Beng Meng Chong ¹, Nur Hawa Nabilah Azman ¹, Muhammad Amirul Aizat Mohd Abdah ¹
and Yusran Sulaiman ^{1,2,*} 

¹ Department of Chemistry, Faculty of Science, Universiti Putra Malaysia, 43400 UPM Serdang, Selangor, Malaysia; c95_beng@hotmail.com (B.M.C.); hawa_nabilah@yahoo.com (N.H.N.A.); amirulaizatabdah93@gmail.com (M.A.A.M.A.)

² Functional Device Laboratory, Institute of Advanced Technology, Universiti Putra Malaysia, 43400 UPM Serdang, Selangor, Malaysia

* Correspondence: yusran@upm.edu.my; Tel.: +60-38-946-6779

Received: 7 January 2019; Accepted: 12 February 2019; Published: 13 March 2019



Featured Application: The potential application of this work is an electrode material for supercapacitor application.

Abstract: Nitrogen-doped graphene (NDG) and mixed metal oxides have been attracting much attention as the combination of these materials resulted in enhanced electrochemical properties. In this study, a composite of nitrogen-doped graphene/manganese oxide/iron oxide (NDG/Mn₃O₄/Fe₃O₄) for a supercapacitor was prepared through the hydrothermal method, followed by freeze-drying. Field emission scanning electron microscopy (FESEM) images revealed that the NDG/Mn₃O₄/Fe₃O₄ composite displayed wrinkled-like sheets morphology with Mn₃O₄ and Fe₃O₄ particles attached on the surface of NDG. The presence of NDG, Mn₃O₄, and Fe₃O₄ was characterized by Fourier transform infrared spectroscopy (FTIR) and X-ray diffraction (XRD). The electrochemical studies revealed that the NDG/Mn₃O₄/Fe₃O₄ composite exhibited the highest specific capacitance (158.46 F/g) compared to NDG/Fe₃O₄ (130.41 F/g), NDG/Mn₃O₄ (147.55 F/g), and NDG (74.35 F/g) in 1 M Na₂SO₄ at a scan rate of 50 mV/s due to the synergistic effect between bimetallic oxides, which provide richer redox reaction and high conductivity. The galvanostatic charge discharge (GCD) result demonstrated that, at a current density of 0.5 A/g, the discharging time of NDG/Mn₃O₄/Fe₃O₄ is the longest compared to NDG/Mn₃O₄ and NDG/Fe₃O₄, indicating that it had the largest charge storage capacity. NDG/Mn₃O₄/Fe₃O₄ also exhibited the smallest resistance of charge transfer (R_{ct}) value (1.35 Ω), showing its excellent charge transfer behavior at the interface region and good cyclic stability by manifesting a capacity retention of 100.4%, even after 5000 cycles.

Keywords: supercapacitor; mixed metal oxides; N-doped graphene

1. Introduction

The rapid growth of the human population and the development of the global economy has caused the increasing demand for energy. The global energy need is predicted to be doubled by the mid-century and more than triple by the end of this century [1]. Therefore, an energy storage system is needed to store excess energy generated and to supply it to electrical devices effectively. Among energy storage devices, supercapacitors are always preferred due to their high performance in energy storage compared to batteries, flywheels, and traditional capacitors. This is because batteries have high energy density, but low power density and short life cycles. In addition to this, flywheels are cost-effective and have a long cycle life, but they have installment and safety issues due to their large size. Traditional capacitors can be charged and discharged in a short time, but they have low energy density.

A supercapacitor is an electrical component that can store a large amount of electrical energy. It is a multicomponent system comprised of two electrodes connected to current collectors and a separator immersed in an electrolyte, and was first used in 1978 as a backup power source in order to maintain computer memory system [2]. Over the years, due to the development of technology, supercapacitors have been widely used in portable electronic devices and hybrid electric vehicles because of their rapid charging-discharging rates, long cycle life, and high specific power. Based on their charge-storage mechanism, supercapacitors are classified into three types: Electrochemical double layer capacitors (EDLCs), pseudocapacitors, and hybrid capacitors.

EDLCs, which are made up of carbon-based materials, store charges electrostatically or non-Faradaically in an electrical double layer formed at the interface between an electrode and electrolyte [3]. Conversely, pseudocapacitors, which consist of transition metal oxides or conducting polymers, accumulate charges through faradic processes in which the charge is transferred across the electrode and electrolyte by reversible redox reaction occurring at the interface [4]. The hybrid capacitor, which is a combination of a EDLC and pseudocapacitor, where both electrical double layer and electrochemical processes are involved in charge storage, enable hybrid capacitors to have the advantages of both EDLCs and pseudocapacitors, i.e., high specific energy and power with good cyclic stability [2].

The materials used in supercapacitor electrodes need to have high conductivity, large surface area, good cyclic stability, and a high theoretical specific capacitance [5]. N-doped graphene (Figure 1) is a good carbon-based electrode material for supercapacitors because it has a large surface area, good cyclic stability, and high electrical conductivity, however, it has low specific capacitance. On the other hand, transition metal oxides such as manganese oxides and iron oxides have high specific capacitance, together with a minimal impact on the environment and low cost, but both of these two oxides have poor cyclic stability and conductivity. Therefore, graphene or N-doped graphene is usually used as a support for transition metal oxides, which provides high electrical conductivity and excellent cyclic stability [6].

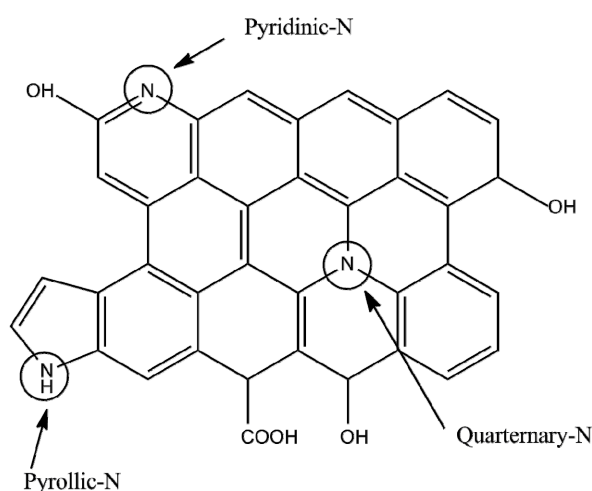


Figure 1. Three common bonding configurations of N atoms in graphene.

Recently, composites of NDG with mixed metal oxides are extensively studied because the incorporation of two metal oxides or bimetallic oxides is believed to possess superior specific capacitance due to the synergistic effect of two types of metal oxides that offer richer redox reactions compared to single metal oxide or spinel oxides, which can give better electrochemical performance. Zhang, et al. [7] synthesized nanocomposites of NDG/ZnO/NiO with a specific capacitance of 1834.9 F/g, which is higher than composites of NDG with single metal oxide because ZnO improved the conductivity of NiO. The nanocomposite has a capacity retention of 93% after 6000 cycles. Ramesh,

et al. [8] reported that NDG/NiO/MnO₂ nanocomposites can achieve a high specific capacitance of 1490 F/g with 98% cyclic stability retention after 2000 cycles.

There are various ways to synthesise NDG/mixed metal oxide composites, such as microwave synthesis, liquid phase plasma, and the solvothermal and hydrothermal method [9]. Among these methods, a hydrothermal method is the most preferred method due to its low cost and simple operation. The hydrothermal process is a process in which the starting materials will be dissolved in the aqueous solvent under high pressure and temperature and then recrystallized into a form of material that is difficult to dissolve under normal conditions. This can give particles that are highly dispersed with the desired size and structure. In addition, only a very small amount and non toxic side product will be produced in the hydrothermal method [2].

In this study, a hybrid material consisting of N-doped graphene (NDG), manganese oxide (Mn₃O₄), and iron oxide (Fe₃O₄) was prepared using by the hydrothermal method, followed by freeze-drying. Hydrazine was chosen as a source of nitrogen to be doped between graphene oxide (GO) sheets and eliminated the oxygenated functional groups of GO in order to restore the conductivity during the hydrothermal process. The supercapacitive performance of N-doped graphene/manganese oxide/iron oxide (NDG/Mn₃O₄/Fe₃O₄) with various iron and manganese salt ratio (Fe:Mn) was thoroughly studied.

2. Materials and Methods

2.1. Chemical and Reagents

Graphene oxide (GO) was purchased from Graphenea (San Sebastian, Spain). Manganese sulphate monohydrate (MnSO₄·H₂O), polytetrafluoroethylene (PTFE), and carbon mesoporous were obtained from Sigma-Aldrich (Steinheim, Germany). Iron sulphate heptahydrate (FeSO₄·7H₂O) and ethanol (95%) were purchased from HmbG (Hamburg, Germany) and John Kollin Corporation (Midlothian, UK), respectively. Sodium sulphate (Na₂SO₄) was obtained from Merck Darmstadt, Germany. Hydrazine monohydrate (N₂H₄·H₂O) and nickel foam was purchased from Nacalai Tesque Inc. (Kyoto, Japan) and Goodfellow (Huntingdon, UK) respectively. Deionized (DI) water was supplied from a Millipore water system (Darmstadt, Germany).

2.2. Preparation of N-Doped Graphene/Metal Oxide (NDG/Metal Oxide) and N-Doped Graphene (NDG)

GO solution (2.67 mg/mL) was first ultrasonicated for 2 h. Then, 25 mM of FeSO₄·7H₂O and 75 mM of MnSO₄·H₂O were added in the homogeneous GO solution and ultrasonicated for 1 hour. After that, the solution was transferred into a 50 mL autoclave and added with 2.5 g of N₂H₄·H₂O. After continuous stirring for 30 minutes, the autoclave was sealed and subjected to hydrothermal reduction at 160 °C for 3 h. The sample was cooled to room temperature and rinsed with DI water several times. Finally, the sample was freeze-dried. NDG was also prepared following the same steps in the absence of FeSO₄·7H₂O and MnSO₄·H₂O.

2.3. Physical Characterization

Field Emission Scanning Electron Microscopy (FESEM) was performed using JEOL JSM-7600F in order to investigate the morphology of the composites. The structural fingerprints of the composites were analyzed via Shimadzu Fourier-transform infrared spectrometer (FTIR), and Shimadzu XRD 6000 diffractometer with Cu K α radiation ($\lambda = 1.54 \text{ \AA}$) at the scan rate of 2 °/min.

2.4. Electrochemical Characterization

The working electrode was prepared by mixing the active material with carbon black and PTFE, which acts as a binder in the ratio of 80:10:10. The mixture was then dispersed in ethanol to form a slurry. The slurry was pasted on a nickel foam (1 cm \times 1 cm) and dried at 60 °C for 12 h. The nickel foam was then subjected to a mechanical pressure of 5 MPa for good attachment between the current

collector and material. The electrochemical characterizations of the composites were conducted using an Autolab (M101) potentiostat with a three-electrode configuration in 1 M Na₂SO₄. Nickel foam, pasted with active materials, was used as a working electrode (WE), platinum wire served as a counter electrode (CE), and silver/silver chloride (Ag/AgCl) served as a reference electrode (RE). Cyclic voltammetry (CV) was performed at a potential range of 0–1 V with various scan rates, i.e., 25, 50, 100, 150, and 200 mV/s, whereas galvanostatic charge–discharge (GCD) was evaluated at different current densities of 0.5, 1.0, 1.5, 2.0, and 2.5 A/g. Electrochemical impedance spectroscopy (EIS) was carried out in the frequency range of 0.1 Hz to 10 kHz at an open circuit potential (OCP) with alternating current (AC) potential at an amplitude of 5 mV. The charge transfer resistance (R_{ct}) and equivalent series resistance (ESR) of the composites were determined from the diameter of the semicircle and the intercept of the semicircle at the Z' axis at the high frequency region of the Nyquist plot, respectively. The cyclic stability test of the composites was performed via CV at a scan rate of 100 mV/s for 5000 cycles.

3. Results and Discussion

3.1. Physical Characterization

Fourier-transform infrared (FTIR) spectroscopy was performed to investigate the chemical structure of NDG, NDG/Fe₃O₄, NDG/Mn₃O₄, and NDG/Mn₃O₄/Fe₃O₄ (Figure 2). In the NDG spectrum (Figure 2a), peaks of N-H stretching, amidic C=O stretching, N-H bending, and C-N stretching can be observed at 3392 cm⁻¹, 1651 cm⁻¹, 1543 cm⁻¹, and 1103 cm⁻¹, respectively. The presence of N-H and C-N in the spectra indicates that nitrogen was successfully doped into graphene oxide during the hydrothermal process. Furthermore, similar peaks of NDG can still be observed in the spectra after the addition of Mn₃O₄ and Fe₃O₄ into NDG, proving a successful anchoring of Mn₃O₄ and Fe₃O₄ on the NDG sheets. In the NDG/Fe₃O₄ spectrum (Figure 2b), two new peaks at 428 cm⁻¹ and 524 cm⁻¹ were noticed, which correspond to Fe-O vibrations. The spectrum of NDG/Mn₃O₄ (Figure 2c) shows the peaks of Mn-O and Mn-O-Mn vibrations at 561 cm⁻¹ and 709 cm⁻¹, respectively. The presence of both metal oxides in the NDG/Mn₃O₄/Fe₃O₄ composite is confirmed by peaks observed at 507 cm⁻¹, 596 cm⁻¹, and 752 cm⁻¹, which correspond to Fe-O, Mn-O, and Mn-O-Mn vibrations, respectively, in the NDG/Mn₃O₄/Fe₃O₄ spectrum (Figure 2d). The peak of Fe-O at 428 cm⁻¹ becomes less visible because it is overlapped with the peak of Fe-O at 507 cm⁻¹.

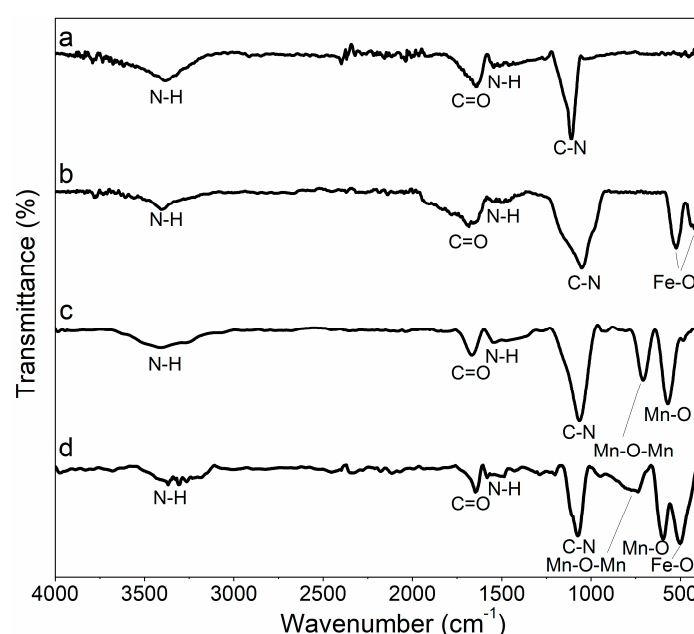


Figure 2. FTIR spectra of (a) NDG, (b) NDG/Fe₃O₄, (c) NDG/Mn₃O₄, and (d) NDG/Mn₃O₄/Fe₃O₄.

Field Emission Scanning Electron Microscopy (FESEM) was performed to investigate the morphologies of NDG, NDG/Fe₃O₄, NDG/Mn₃O₄, and NDG/Mn₃O₄/Fe₃O₄. As shown in Figure 3a, NDG exhibits a wrinkle-like sheet morphology, which can also be noticed in the FESEM images of NDG/Fe₃O₄, NDG/Mn₃O₄, and NDG/Mn₃O₄/Fe₃O₄ (Figure 3b–d). After the addition of Fe₃O₄, the well-dispersed particles of Fe₃O₄ can be clearly seen to cover the surface of wrinkled NDG sheets (Figure 3b). The presence of Mn₃O₄ in NDG/Mn₃O₄ (Figure 3c) is confirmed as Mn₃O₄ particles that obviously attach on the NDG sheets. Upon the addition of both Fe₃O₄ and Mn₃O₄ into NDG, a large number of Fe₃O₄ and Mn₃O₄ particles can be seen anchored on the wrinkled surface of NDG, indicating that both metal oxides are successfully added into NDG (Figure 3d). The presence of the dispersed particles of Fe₃O₄ and Mn₃O₄ cover on the surface of NDG sheets have enhanced C_{sp} of the composites due to their highly pseudocapacitive properties [10]. This could be due to the presence of Fe₃O₄ and Mn₃O₄ particles on the wrinkle NDG sheets, which effectively prevent severe agglomeration of NDG sheets [11] and provide more accessible sites for the electrochemical reaction.

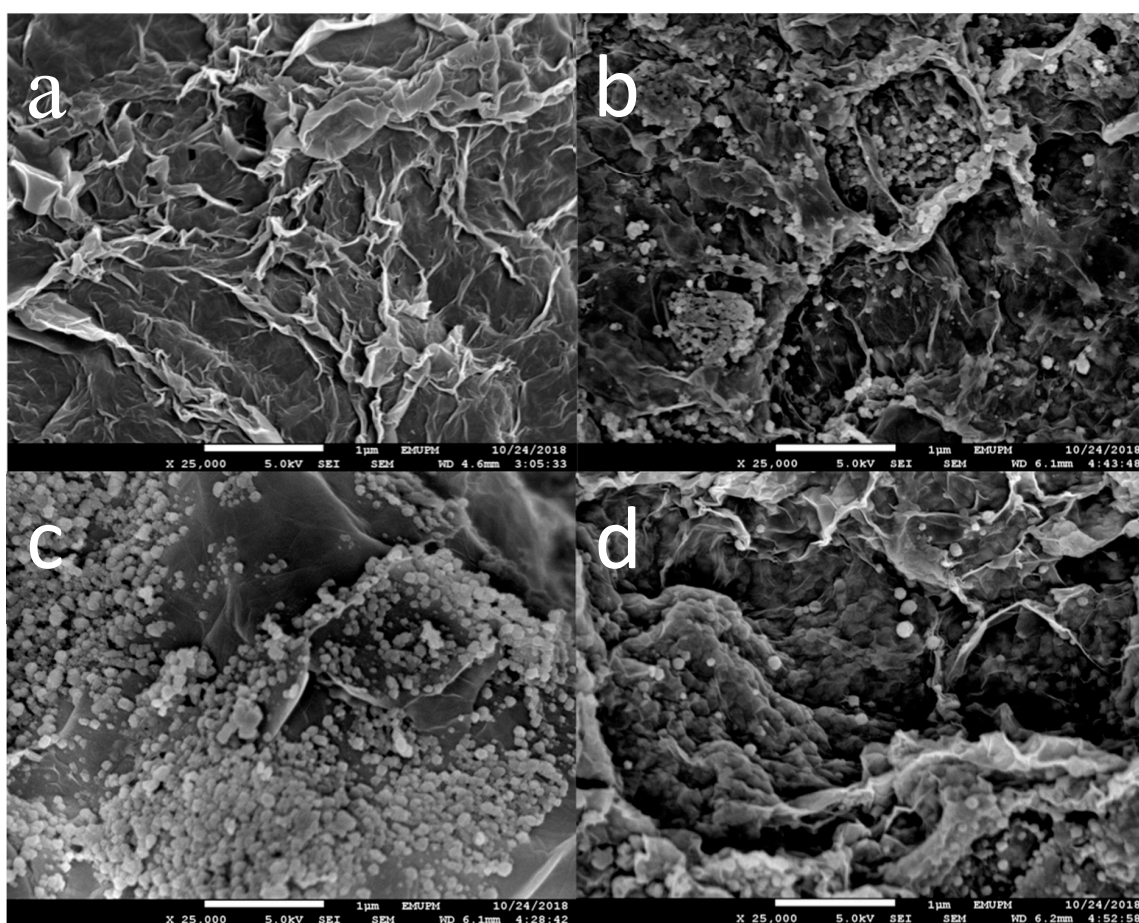


Figure 3. Field Emission Scanning Electron Microscopy (FESEM) images of (a) NDG, (b) NDG/Fe₃O₄, (c) NDG/Mn₃O₄, and (d) NDG/Mn₃O₄/Fe₃O₄.

X-ray diffraction (XRD) was performed to identify the structure and crystallinity of the prepared NDG, NDG/Fe₃O₄, NDG/Mn₃O₄, and NDG/Mn₃O₄/Fe₃O₄. In Figure 4a, the large broad peak at 24.6°, corresponding to the (002) plane, indicates the disordered arrangement of loosely packed graphene sheets of NDG [12]. The diffraction peaks of NDG are less visible in the XRD patterns of NDG/Fe₃O₄, NDG/Mn₃O₄, and NDG/Mn₃O₄/Fe₃O₄ due to the relatively small diffraction intensity of NDG compared to the strong peaks of Fe₃O₄ and Mn₃O₄ [13]. For NDG/Fe₃O₄ (Figure 4b), the peaks observed at 30.2°, 35.5°, 43.2°, 57.1°, 62.7°, and 74.2° are related to the (220), (311), (400), (511), (440), and (533) planes of the Fe₃O₄ cubic crystalline system (JCPDS 01-088-0315). The peaks observed

at 18.0°, 32.5°, 36.2°, 38.1°, 44.6°, 58.8°, and 60.0° in the XRD pattern of NDG/Mn₃O₄ (Figure 4c) corresponds to the (101), (103), (211), (004), (220), (321), and (224) planes of tetragonal crystallinity in Mn₃O₄ (JCPDS 00-001-1127). For NDG/Mn₃O₄/Fe₃O₄, almost all the characteristic peaks for Fe₃O₄ and Mn₃O₄ can be observed (Figure 4d), confirming that both Fe₃O₄ and Mn₃O₄ exist in the composite. The diffraction peaks of Fe₃O₄ in NDG/Mn₃O₄/Fe₃O₄ shift to a lower angle, as compared to NDG/Fe₃O₄, indicating a partial change of the lattice structure of Fe₃O₄ after the addition of Mn₃O₄ [7].

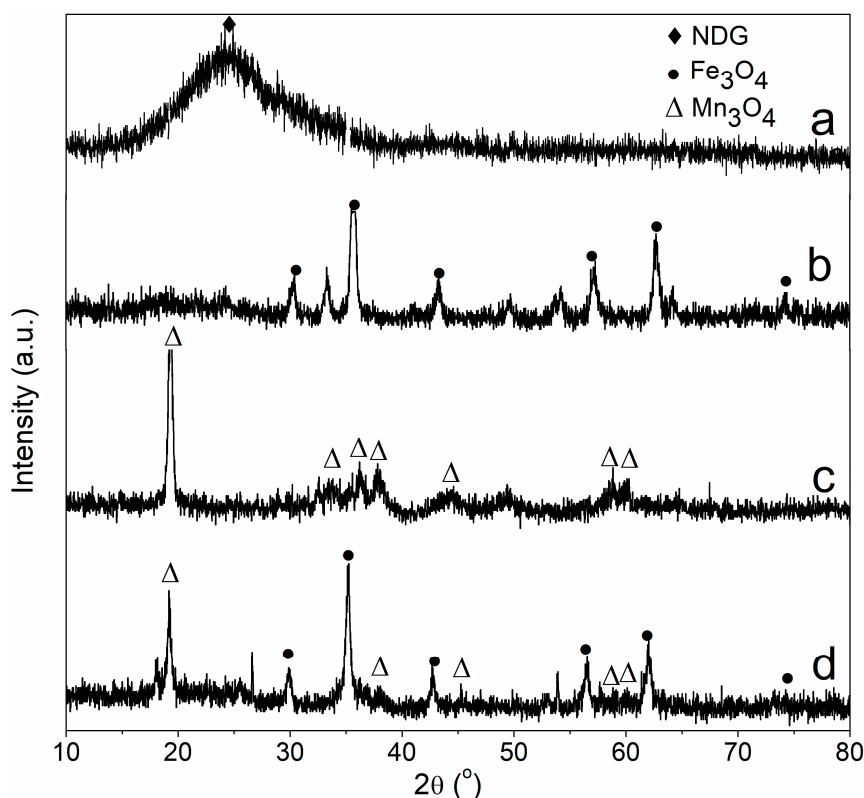


Figure 4. XRD patterns of (a) NDG, (b) NDG/Fe₃O₄, (c) NDG/Mn₃O₄, and (d) NDG/Mn₃O₄/Fe₃O₄.

3.2. Electrochemical Characterization

Cyclic voltammetry (CV) was performed in 1 M Na₂SO₄ to evaluate the capacitive performance of prepared NDG, NDG/Mn₃O₄, NDG/Fe₃O₄, and NDG/Mn₃O₄/Fe₃O₄ as electrode materials for a supercapacitor. The specific capacitance (C_{sp}) of the composites was calculated using Equation (1):

$$C_{sp} = \frac{\int IdV}{mv\Delta V} \quad (1)$$

where I is the current density (A/g), v is the scan rate applied (mV/s), ΔV is the potential range applied, and m is the mass of the sample (g). Figure 5a shows the CV curves of NDG/Mn₃O₄/Fe₃O₄ with a different ratio of Fe:Mn at a scan rate of 50 mV/s. NDG/Mn₃O₄/Fe₃O₄ with the Fe:Mn ratio of 1:3 exhibits the highest C_{sp} (158.46 F/g) compared to ratios of 1:0 (130.41 F/g), 3:1 (74.16 F/g), 1:1 (82.05 F/g), and 0:1 (147.55 F/g), as the composite has the largest enclosed area of the CV curve. The C_{sp} of NDG/Mn₃O₄/Fe₃O₄ with a Fe:Mn ratio of 1:3 is higher than the Fe:Mn ratio of 3:1, suggesting that the Mn-based species contribute in the major part of the charge storage mechanism, while Fe species serve as a synergist to enhance the capacitance when both species are mixed together [7]. Quasi-rectangular CV curves and small humps are observed for NDG/Mn₃O₄/Fe₃O₄ in all Fe:Mn ratios, NDG/Fe₃O₄, and NDG/Mn₃O₄ (Figure 5b), which indicate that the capacitance is mainly contributed by Faradaic pseudocapacitance [14], which is contributed by the metal oxides [15].

NDG/Mn₃O₄/Fe₃O₄ exhibits the largest enclosed CV curve area, indicating that it has the highest C_{sp} (158.46 F/g) compared to NDG, NDG/Fe₃O₄, and NDG/Mn₃O₄. This might be due to the presence of both Fe₃O₄ and Mn₃O₄ that enhance the pseudocapacitance of the composites. In addition, bimetallic oxides provide richer redox reactions compared to single metallic oxide, and thus help to further improve the capacitive performance of the composites [16]. NDG/Fe₃O₄ and NDG/Mn₃O₄ exhibit higher C_{sp} compared to NDG because the dispersion of metal oxides between N-doped graphene sheets prevents the sheets from restacking to increase the number of accessible sites for electrolyte ions [17].

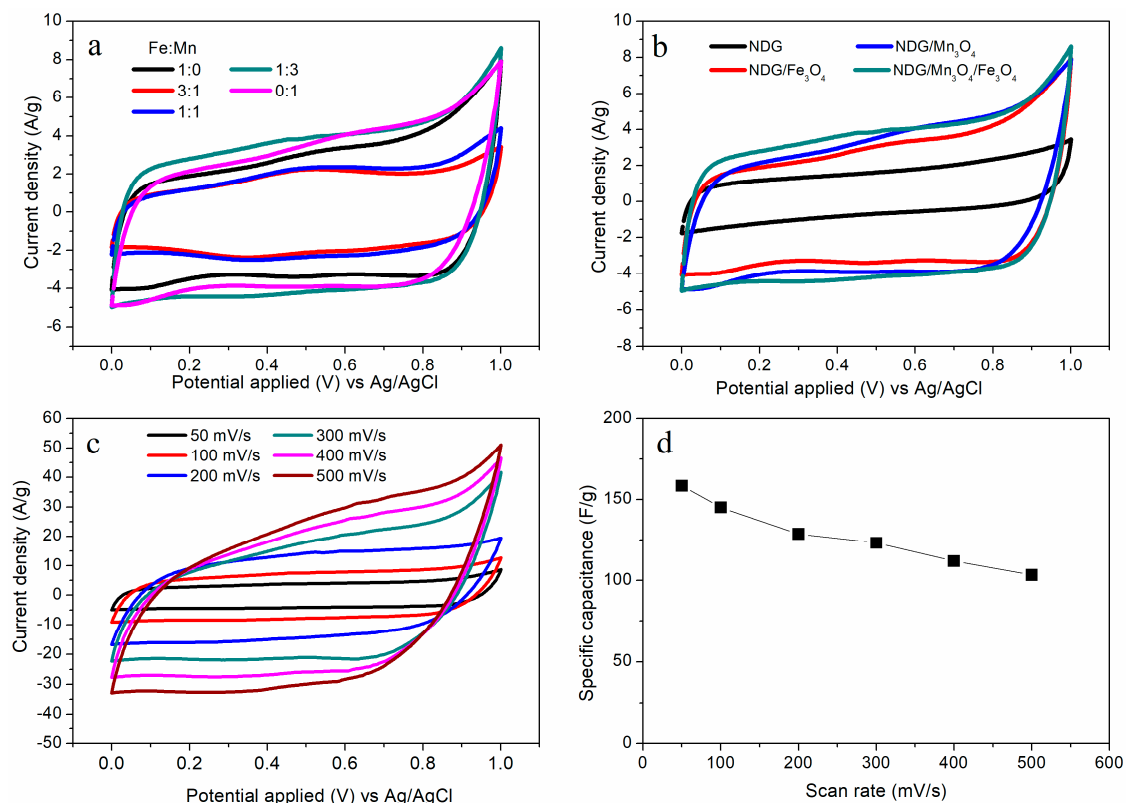


Figure 5. (a) CV curves of NDG/Mn₃O₄/Fe₃O₄ with Fe:Mn ratio of 1:0, 3:1, 1:1, 1:3, and 0:1 in 1.0 M Na₂SO₄ at a scan rate of 50 mV/s. (b) CV curves of NDG, NDG/Fe₃O₄, NDG/Mn₃O₄, and NDG/Mn₃O₄/Fe₃O₄ in 1.0 M Na₂SO₄ at a scan rate of 50 mV/s. (c) CV curves of NDG/Mn₃O₄/Fe₃O₄. (d) Calculated specific capacitance of NDG/Mn₃O₄/Fe₃O₄ with various scan rates.

The effect of the scan rate on the capacitive performance of NDG/Mn₃O₄/Fe₃O₄ was studied between 50 and 500 mV/s. As can be seen in Figure 5c, there is a little distortion of the quasi-rectangular shape CV curves at a high scan rate of 500 mV/s. The C_{sp} values (Figure 5d) decline from 158.46 F/g to 128.74 F/g as the scan rate increases from 50 mV/s to 500 mV/s, with 65.22% of the initial C_{sp} retained. This is because the diffusion of electrolyte ions to the electrode surface becomes limited with time constraints as the scan rate increases [18].

Galvanostatic charge/discharge (GCD) was carried out to further investigate the capacitive performance of the prepared NDG/Mn₃O₄, NDG/Fe₃O₄, and NDG/Mn₃O₄/Fe₃O₄. As shown in Figure 6, all the GCD curves show a nearly symmetrical triangular shape with only a small deviation from linearity due to the contribution from the pseudocapacitance [9]. In addition, insignificant voltage drop (IR drop) in the GCD curves of NDG/Mn₃O₄/Fe₃O₄, NDG/Mn₃O₄, and NDG/Fe₃O₄ (Figure 6a) show high efficiency of ion transport or diffusion near the electrode–electrolyte interface [19]. IR drops occur during the charge/discharge process due to internal resistance, which includes the boundary resistance of electrode/electrolyte and the contact resistance between the active material and current collector [20]. Hence, a small IR drop indicates low internal resistance, which leads to a high power

density [18]. From the GCD curves, the specific capacitance of the composites can be calculated according to Equation (2):

$$C_{sp} = \frac{I\Delta t}{m\Delta V} \quad (2)$$

where C_{sp} is the specific capacitance of the electrode (F/g), Δt is the discharging time (s), I is the discharge current (A/g), ΔV is the potential range (V), and m is the mass of the electrode material (g). NDG/Mn₃O₄/Fe₃O₄ exhibits the highest C_{sp} (90.58 F/g), followed by NDG/Mn₃O₄ (83.21 F/g) and NDG/Fe₃O₄ (14.27 F/g). NDG/Mn₃O₄/Fe₃O₄ also shows the longest discharge time, as compared to NDG/Mn₃O₄ and NDG/Fe₃O₄ at 0.5 A/g (Figure 6a), indicating that NDG/Mn₃O₄/Fe₃O₄ possesses the highest charge storage capacity [8,21]. The discharging time of NDG/Mn₃O₄/Fe₃O₄ becomes shorter as current density increases from 0.5 A/g to 2.5 A/g (Figure 6b), indicating the decrease of C_{sp} from 90.58 F/g to 73.10 F/g. The decrease of C_{sp} is caused by faster ion migration at a higher current density, which accelerates the polarisation and depolarisation process of the electrode. This will result in the incomplete utilisation of ions on the electrode surface [22].

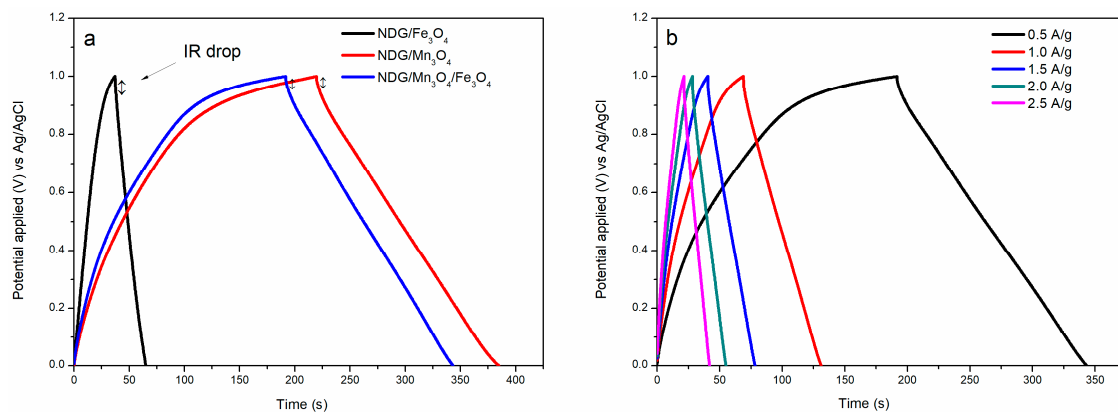


Figure 6. GCD curves of (a) NDG/Fe₃O₄, NDG/Mn₃O₄, and NDG/Mn₃O₄/Fe₃O₄ at a current density of 0.5 A/g and (b) NDG/Mn₃O₄/Fe₃O₄ at different current densities: 0.5 A/g, 1.0 A/g, 1.5 A/g, 2.0 A/g, and 2.5 A/g.

Electrochemical impedance spectroscopy (EIS) was performed to evaluate the resistive behavior of all the composites. Nyquist plots of NDG/Mn₃O₄, NDG/Fe₃O₄, and NDG/Mn₃O₄/Fe₃O₄ (Figure 7) consist of a semicircle in the high frequency region and a vertical line in the low frequency region. The vertical line in the low frequency region of Nyquist plots for all the composites approach 90°, suggesting rapid ion transport between the electrode and electrolyte and ideal capacitive behavior [23]. The diameter of the semicircle is related to R_{ct} at the electrode–electrolyte interface. NDG/Mn₃O₄/Fe₃O₄ possesses the smallest diameter of the semicircle, followed by NDG/Mn₃O₄ and NDG/Fe₃O₄, indicating that NDG/Mn₃O₄/Fe₃O₄ has the lowest R_{ct} (1.35 Ω), as compared to NDG/Mn₃O₄ (1.39 Ω) and NDG/Fe₃O₄ (1.49 Ω). This suggests that NDG with bimetallic oxides have a lower contact resistance and the greater charge transfer rate at the electrode–electrolyte interface compared to NDG with single metal oxides [24]. At the high frequency region, the intercept of the semicircle at the Z' axis gives information about equivalent series resistance (ESR), which is the combination of the internal resistance of the electroactive materials, the interfacial resistance between the electrode and the current collector, and the intrinsic ionic electrolyte resistance [25]. The ESR values of NDG/Mn₃O₄/Fe₃O₄, NDG/Fe₃O₄, and NDG/Mn₃O₄ are 3.61 Ω, 3.87 Ω, and 4.65 Ω, respectively, as shown in Table 1. NDG/Mn₃O₄/Fe₃O₄ exhibits the lowest ESR value, demonstrating that the composite has the lowest contact resistance at the interface of active material and a current collector, which contributes to rapid ion diffusion [11]. The low ESR value also proves the lowest internal resistance in NDG/Mn₃O₄/Fe₃O₄, which is supported by an insignificant iR drop observed in the GCD curve [14]. These EIS results also agree well with the CV results.

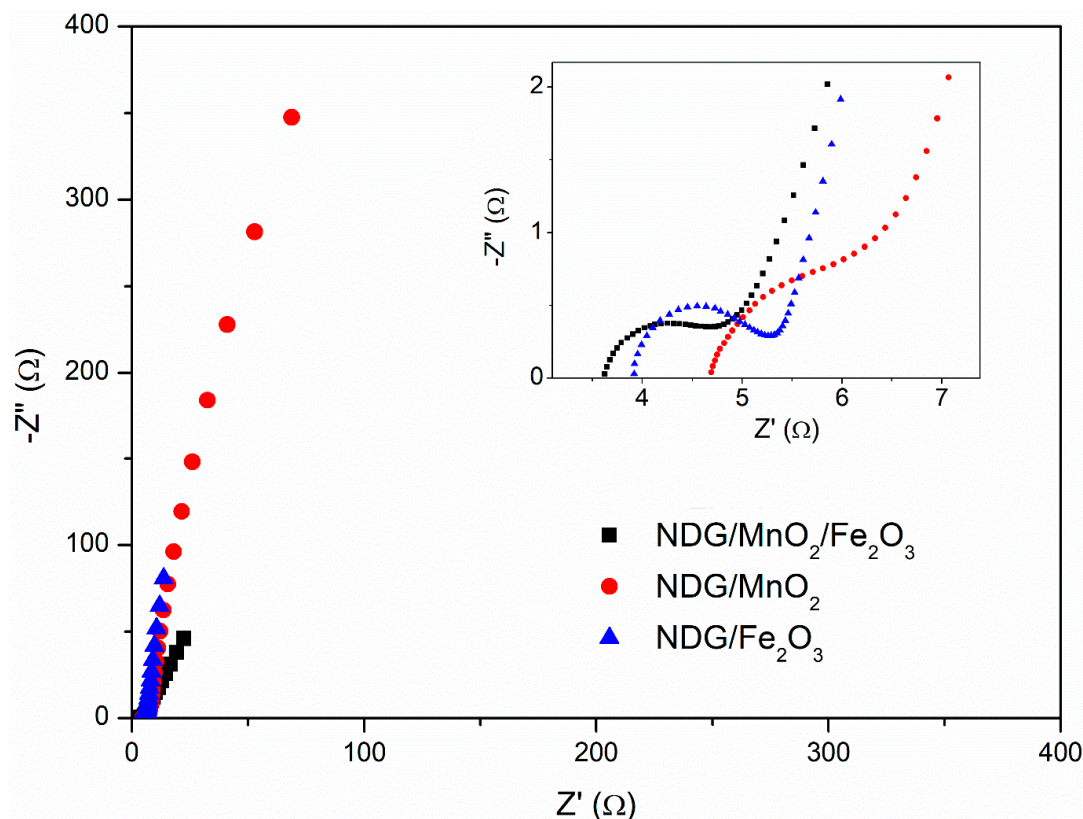


Figure 7. Nyquist plots of NDG/Mn₃O₄, NDG/Fe₃O₄, and NDG/Mn₃O₄/Fe₃O₄ (the inset is the magnified Nyquist plots of NDG/Mn₃O₄, NDG/Fe₃O₄, and NDG/Mn₃O₄/Fe₃O₄ at the high-frequency range).

Table 1. The values of R_{ct} and ESR of NDG/Mn₃O₄, NDG/Fe₃O₄, and NDG/Mn₃O₄/Fe₃O₄.

Samples	R_{ct} (Ω)	ESR (Ω)
NDG/Mn ₃ O ₄	1.39	4.65
NDG/Fe ₃ O ₄	1.49	3.87
NDG/Mn ₃ O ₄ /Fe ₃ O ₄	1.35	3.61

Cyclic stability tests were carried out at a scan rate of 100 mV/s for 5000 cycles to evaluate the capacitance retention of NDG/Mn₃O₄/Fe₃O₄. As shown in Figure 8a, the C_{sp} retention of NDG/Mn₃O₄/Fe₃O₄ initially increases until the 2500th cycle, and then decreases to 103.4% at the 5000th cycle. The initial increase in capacitance of NDG/Mn₃O₄/Fe₃O₄ may be due to the active site activation of the composites [10,26]. After activation, the electrochemically active materials will be completely exposed to the electrolyte [27]. This phenomenon can be related to the ESR value of the composite after 2500 cycles (Figure 8b), in which the ESR decreases to 1.83 Ω due to the proper wetting of the electrode surface, which can enhance the electrolyte diffusion. From 2500 to 5000 cycles, there is an decrease in C_{sp} retention that was caused by activity loss of the metal oxide particles during the charging and discharging processes [26]. This phenomenon is also supported by the EIS data, in which there is an increase in ESR (2.12 Ω). Generally, the NDG/Mn₃O₄/Fe₃O₄ shows good cyclic stability due to the strong bonding between dispersed metal oxide particles and NDG with high mechanical strength, which can effectively prevent the volume expansion and aggregation of metal oxides during the charging and discharging processes [7,28]. The cycling stability of NDG/Mn₃O₄/Fe₃O₄ is higher in comparison to MnFe₂O₄/graphene reported in the literature [11].

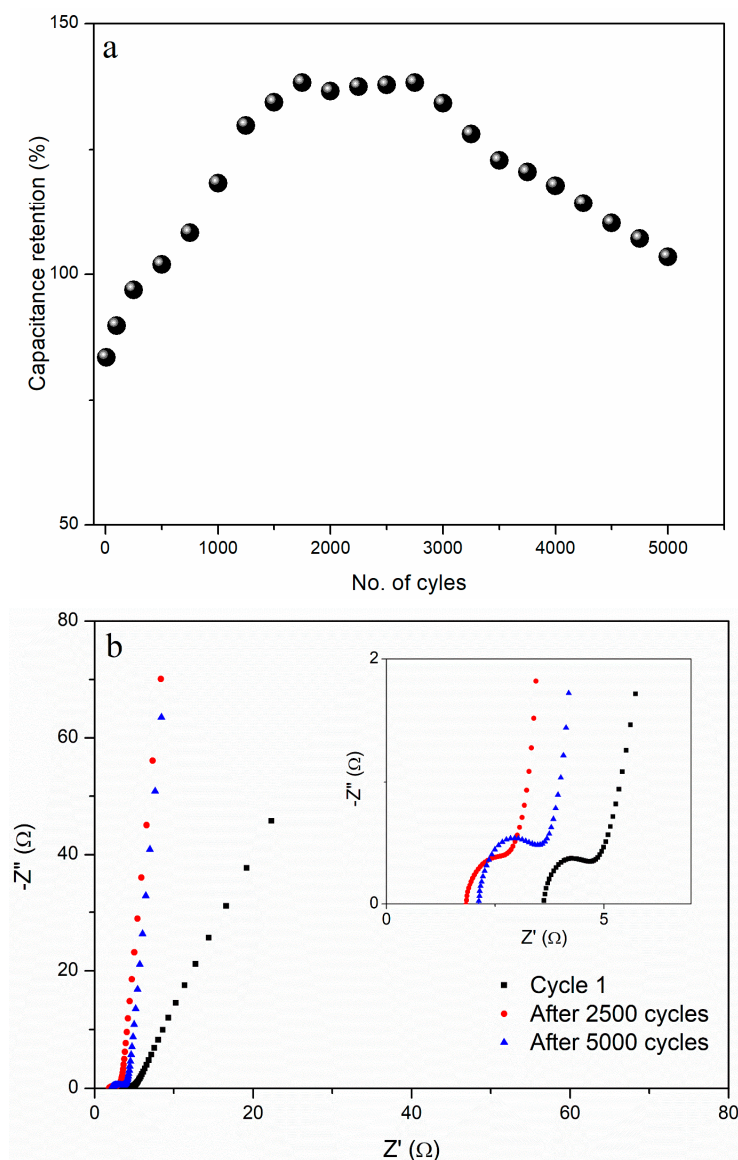


Figure 8. (a) Capacitance retention of NDG/Mn₃O₄/Fe₃O₄ in 1.0 M Na₂SO₄ at a scan rate of 100 mV/s for 5000 cycles and (b) Nyquist plot of NDG/Mn₃O₄/Fe₃O₄ after cyclic stability test in 1.0 M Na₂SO₄ (the inset is the magnified Nyquist plots of NDG/Mn₃O₄/Fe₃O₄ at the high-frequency range).

4. Conclusions

NDG/Mn₃O₄/Fe₃O₄ with different Fe:Mn ratios were successfully prepared using a hydrothermal method followed by freeze-drying. The combination of the high conductivity of NDG with richer redox reaction from Mn₃O₄/Fe₃O₄ resulted in the enhanced electrochemical performance of the composite with bimetallic oxide compared to the composite with a single metal oxide, which is due to Mn₃O₄ and Fe₃O₄ particles being attached on the wrinkled surface of NDG that helped to prevent agglomeration of the NDG sheets. Different Fe:Mn ratios in NDG/Mn₃O₄/Fe₃O₄ were studied and the results showed that the ratio between the metal oxides also played an important role in enhancing the supercapacitive performance of the composite. The Fe:Mn ratio of 1:3 exhibited the highest specific capacitance and had excellent cyclic stability with the lowest R_{ct} and ESR value, which indicates good energy storing ability, a superior life cycle, and fast charge transfer at the electrode–electrolyte interface. Therefore, NDG/Mn₃O₄/Fe₃O₄ is a potential material for electrodes to be used in supercapacitors.

Author Contributions: B.M.C. performed the experiments and analyzed the data. B.M.C., N.H.N.A., and Y.S. wrote the paper. M.A.A.M.A. provided helpful discussion in order to improve the manuscript. Y.S. supervised and gave guidance on the experimental design, analyzing data, and writing the manuscript.

Funding: This research was funded by the Ministry of Education, Malaysia through the Fundamental Research Grant Scheme (01-02-13-1388FR).

Acknowledgments: The authors would like to thank Universiti Putra Malaysia for the laboratory facilities.

Conflicts of Interest: The authors declare no conflict of interest.

References

1. Yan, J.; Wang, Q.; Wei, T.; Fan, Z. Recent Advances in Design and Fabrication of Electrochemical Supercapacitors with High Energy Densities. *Adv. Energy Mater.* **2014**, *4*, 1300816. [[CrossRef](#)]
2. Kate, R.S.; Khalate, S.A.; Deokate, R.J. Overview of nanostructured metal oxides and pure nickel oxide (NiO) electrodes for supercapacitors: A review. *J. Alloy. Compd.* **2018**, *734*, 89–111. [[CrossRef](#)]
3. Djuric, S.M.; Kitic, G.; Dubourg, G.; Gajic, R.; Tomasevic-Ilic, T.; Minic, V.; Spasenovic, M. Miniature graphene-based supercapacitors fabricated by laser ablation. *Microelectron. Eng.* **2017**, *182*, 1–7. [[CrossRef](#)]
4. Wang, K.; Xu, M.; Gu, Y.; Gu, Z.; Liu, J.; Fan, Q.H. Low-temperature plasma exfoliated n-doped graphene for symmetrical electrode supercapacitors. *Nano Energy* **2017**, *31*, 486–494. [[CrossRef](#)]
5. Bose, S.; Kuila, T.; Mishra, A.K.; Rajasekar, R.; Kim, N.H.; Lee, J.H. Carbon-based nanostructured materials and their composites as supercapacitor electrode. *J. Mater. Chem.* **2012**, *22*, 767–784. [[CrossRef](#)]
6. Wang, P.; Sun, S.; Wang, S.; Zhang, Y.; Zhang, G.; Li, Y.; Li, S.; Zhou, C.; Fang, S. Ultrastable MnO₂ nanoparticle/three-dimensional N-doped reduced graphene oxide composite as electrode material for supercapacitor. *J. Appl. Electrochem.* **2017**, *47*, 1293–1303. [[CrossRef](#)]
7. Zhang, M.; Ma, T.; Wang, Y.; Pan, D.; Xie, J. Microwave synthesis of three dimensional N-doped graphene self-supporting networks coated with Zinc/Nickel oxide nanocrystals for supercapacitor electrode applications. *J. Mater. Sci. Mater. Electron.* **2018**. [[CrossRef](#)]
8. Ramesh, S.; Karuppasamy, K.; Msolli, S.; Kim, H.-S.; Kim, H.S.; Kim, J.-H. A nanocrystalline structured NiO/MnO₂@nitrogen-doped graphene oxide hybrid nanocomposite for high performance supercapacitors. *New J. Chem.* **2017**, *41*, 15517–15527. [[CrossRef](#)]
9. Chen, G.Z. Understanding supercapacitors based on nano-hybrid materials with interfacial conjugation. *Prog. Nat. Sci. Mater. Int.* **2013**, *23*, 245–255. [[CrossRef](#)]
10. Zhao, C.; Shao, X.; Zhang, Y.; Qian, X. Fe₂O₃/RGO/Fe₃O₄ Composite in-situ Grown on Fe Foil for High performance Supercapacitors. *ACS Appl. Mater. Interfaces* **2016**, *8*, 30133–30142. [[CrossRef](#)] [[PubMed](#)]
11. Cai, W.; Lai, T.; Dai, W.; Ye, J. A facile approach to fabricate flexible all-solid-state supercapacitors based on MnFe₂O₄/graphene hybrids. *J. Power Sources* **2014**, *255*, 170–178. [[CrossRef](#)]
12. Elsiddig, Z.A.; Wang, D.; Xu, H.; Zhang, W.; Zhang, T.; Zhang, P.; Tian, W.; Sun, Z.; Chen, J. Three-dimensional nitrogen-doped graphene wrapped LaMnO₃ nanocomposites as high-performance supercapacitor electrodes. *J. Alloy. Compd.* **2018**, *740*, 148–155. [[CrossRef](#)]
13. Ma, X.; Zhang, P.; Zhao, Y.; Liu, Y.; Li, J.; Zhou, J.Y.; Pan, X.; Xie, E. Role of N doping on the electrochemical performances of ZnCo₂O₄ quantum dots/reduced graphene oxide composite nanosheets. *Chem. Eng. J.* **2017**, *327*, 1000–1010. [[CrossRef](#)]
14. Liu, Y.; He, D.; Wu, H.; Duan, J.; Zhang, Y. Hydrothermal Self-assembly of Manganese Dioxide/Manganese Carbonate/Reduced Graphene Oxide Aerogel for Asymmetric Supercapacitors. *Electrochim. Acta* **2015**, *164*, 154–162. [[CrossRef](#)]
15. Kuo, S.-L.; Wu, N.-L. Electrochemical Capacitor of MnFe₂O₄ with NaCl Electrolyte. *Electrochem. Solid-State Lett.* **2005**, *8*, A495. [[CrossRef](#)]
16. Azman, N.H.N.; Mamat Mat Nazir, M.S.; Ngee, L.H.; Sulaiman, Y. Graphene-based ternary composites for supercapacitors. *Int. J. Energy Res.* **2018**, *42*, 2104–2116. [[CrossRef](#)]
17. Goljanian Tabrizi, A.; Arsalani, N.; Mohammadi, A.; Namazi, H.; Saleh Ghadimi, L.; Ahadzadeh, I. Facile synthesis of a MnFe₂O₄/rGO nanocomposite for an ultra-stable symmetric supercapacitor. *New J. Chem.* **2017**, *41*, 4974–4984. [[CrossRef](#)]
18. Mohd Abdah, M.A.A.; Zubair, N.A.; Azman, N.H.N.; Sulaiman, Y. Fabrication of PEDOT coated PVA-GO nanofiber for supercapacitor. *Mater. Chem. Phys.* **2017**, *192*, 161–169. [[CrossRef](#)]

19. Yue, F.; Zheng, Y.; Liu, J.; Song, X.; Wang, H.; Li, F.; Tian, Y.; Zhang, J.; Hou, S. Scalable Synthesis of High-Tapped-Density N-doped Graphene by Polyethyleneimine-Mediated Thermal Treatment of Graphene Oxide and Its Application for Supercapacitors. *Electrochim. Acta* **2017**, *254*, 181–190. [[CrossRef](#)]
20. Tseng, L.-H.; Hsiao, C.-H.; Nguyen, D.D.; Hsieh, P.-Y.; Lee, C.-Y.; Tai, N.-H. Activated carbon sandwiched manganese dioxide/graphene ternary composites for supercapacitor electrodes. *Electrochim. Acta* **2018**, *266*, 284–292. [[CrossRef](#)]
21. Li, J.; Chen, Y.; Wu, Q.; Xu, H. Synthesis and electrochemical properties of Fe₃O₄/MnO₂/RGOs sandwich-like nano-superstructures. *J. Alloy. Compd.* **2017**, *693*, 373–380. [[CrossRef](#)]
22. Singh, S.K.; Dhavale, V.M.; Boukherroub, R.; Kurungot, S.; Szunerits, S. N-doped porous reduced graphene oxide as an efficient electrode material for high performance flexible solid-state supercapacitor. *Appl. Mater. Today* **2017**, *8*, 141–149. [[CrossRef](#)]
23. Zhu, J.; Tang, S.; Xie, H.; Dai, Y.; Meng, X. Hierarchically porous MnO₂ microspheres doped with homogeneously distributed Fe₃O₄ nanoparticles for supercapacitors. *ACS Appl Mater Interfaces* **2014**, *6*, 17637–17646. [[CrossRef](#)] [[PubMed](#)]
24. Si, P.; Ding, S.; Lou, X.-W.; Kim, D.-H. An electrochemically formed three-dimensional structure of polypyrrole/graphene nanoplatelets for high-performance supercapacitors. *RSC Adv.* **2011**, *1*, 1271. [[CrossRef](#)]
25. Sankar, K.V.; Selvan, R.K. The preparation of MnFe₂O₄ decorated flexible graphene wrapped with PANI and its electrochemical performances for hybrid supercapacitors. *RSC Adv. Pap.* **2014**, *4*, 17555–17566. [[CrossRef](#)]
26. Ren, R.; Faber, M.S.; Dziejczak, R.; Wen, Z.; Jin, S.; Mao, S.; Chen, J. Metallic CoS₂ nanowire electrodes for high cycling performance supercapacitors. *Nanotechnology* **2015**, *26*, 494001. [[CrossRef](#)] [[PubMed](#)]
27. Gao, Z.; Wang, J.; Li, Z.; Yang, W.; Wang, B.; Hou, M.; He, Y.; Liu, Q.; Mann, T.; Yang, P.; et al. Graphene Nanosheet/Ni²⁺/Al³⁺ Layered Double-Hydroxide Composite as a Novel Electrode for a Supercapacitor. *Chem. Mater.* **2011**, *23*, 3509–3516. [[CrossRef](#)]
28. Li, L.; Hu, Z.; Yang, Y.; Liang, P.; Lu, A.; Xu, H.; Hu, Y.; Wu, H. Hydrothermal Self-assembly Synthesis of Mn₃O₄/Reduced Graphene Oxide Hydrogel and Its High Electrochemical Performance for Supercapacitors. *Chin. J. Chem.* **2013**, *31*, 1290–1298. [[CrossRef](#)]



© 2019 by the authors. Licensee MDPI, Basel, Switzerland. This article is an open access article distributed under the terms and conditions of the Creative Commons Attribution (CC BY) license (<http://creativecommons.org/licenses/by/4.0/>).